1250–1257 Vol. 78 No. 6 ACTA GEOLOGICA SINICA Dec. 2004
http://www.geojournals.cn/dzxbcn/ch/index.aspx

An Inverse Analysis of the Comprehensive Medium Parameters and a Simulation of the Crustal Deformation of the Qinghai-Tibet Plateau

LI Tianwen[1,2], CHEN Jianbing[3], TANG Guo'an[1,2], WU Lin[2] and LI Junfeng[2]
1 *Continental Movement Dynamics Lab, Northwest University, Xi'an, Shannxi 710069; E-mail: tianwenli@126.com*
2 *Department of Urban and Resource, Northwest University, Xi'an, Shannxi 710069*
3 *Cold Region Road Engineering Institute, the First Highway Survey and Design Institute; Xi'an, Shaanxi 710069*

Abstract Based on the theory of finite element analysis, an inverse analysis model for the comprehensive medium parameters of the Qinghai-Tibet Plateau is set up. With the help of GPS velocity field, the comprehensive crustal medium parameters of the plateau are inversely analyzed and the characteristics of the related movement macroscopically simulated. It is then concluded that the tectonic deformation of the plateau is mainly in the form of a N-S compression accompanied by an E-W stretching, and the present tectonic setting of the plateau should be the result of the collision between the Indian and the Eurasian continents during the Cenozoic.

Key words: Qinghai-Tibet Plateau, medium parameter, inverse analysis on displacement, simulation, tectonic deformation

1 Introduction

The Qinghai-Tibet Plateau, "the roof of the earth", is a gigantic tectonic unit of the top altitude on earth. Its elevation has been one of the significant natural events on the Asian continent since the Cenozoic. China is endowed with unique geological conditions for the research on this continental deformation. The Qinghai-Tibet Plateau and its surrounding mountains form up a structural strip of continental geology, which is of the most typical sense the world over, providing us with the best natural laboratory for the research on the deformation of the continental crust (Armijo et al., 1986; Sino-British Comprehensive Geological Investigation Team of the Qinghai-Tibet Plateau, 1990; Hou et al., 2002; Wu et al., 2004). The geological structure in the area stretching from Lhasa through Tingri and Rongpu Temple to the 87° longitude is quite complicated because it is not only the suture between the Indian and Eurasian continents, but an area of fairly violent plate movement and topographical rises and falls as well. Thus, it is of great significance not only theoretically but also practically for the prediction of mineral resources (Gao et al., 2003) and earthquakes (Yang et al., 2003) and protection of the environment and mitigation of natural disasters, to precisely monitor crustal changes with the GPS technique and to explore the changing mechanism of the continental lithosphere to set up our new theory on continental geological structures in this unique geologicial area (Bilham et al., 1997; Blisniuk et al., 1998; Yang and Ju, 1999; Jin and Zhu, 2003).

It is absolutely necessary to set up an inverse analysis model of plateau crustal deformation and displacement on the basis of the geological background and its dynamic mechanism of the crustal movement on the Qinghai-Tibet Plateau with the help of geodetic survey data (3-D spatial coordinates). Setting up the model aims at the following purposes: (1) to estimate the dynamic characteristics of the plateau crust and (2) to find out the driving force of the plateau crustal changes to make rational predictions of the plateau crustal movement to further the research on the global plate movement.

With the development of the computing technique, mutual supplement between physical experiments and data computation has become a new research frame of earth science. Wang Ren used the linear stacking principle to inversely analyze the stress field in east Asia (Wang, 1989); Zhang Dongning and Xu Zhonghuai used the finite element to inversely analyze the functional forces in the east part of Chinese continent and its nearby boundaries (Zhang et al., 1994); and recently, Wang Suyun used the slide technique to inversely analyze the force of the Chinese continent and its neighboring plates (Wang et al., 1996); Yang Yuanxi used the finite element difference technique to inversely analyze the material parameters of well-distributed media (Yang, 1991), and Yan Renjun et al. put forward a resolution counting technique of inverse media in the area (Yan, 1998). However, due to the limitations of the used techniques and the computers' capability, the above researches are confined to be static or pseudo static and two-dimensional.

This paper focuses on estimating the dynamic characteristic parameters of the crust in the Qinghai-Tibet Plateau, namely on inversely analyzing the comprehensive medium parameters of the plateau. The search for the driving force of the crustal deformation in the plateau or the inverse analysis on the boundary functional forces will be discussed in another paper.

2 An Inverse Analysis Model for the Medium Parameters

A medium parameter usually refers to the minimum error between the factual structural deformation and the actually measured one when there is such a parameter or Poisson's ratio in the medium. In practice, due to the complexity of the crust, it is very difficult to set up a model that can fully reflect the characteristics of the crustal rock. If the model is too complicated, it will be impossible to get the solution. Therefore, to use the GPS velocity field to get the related physical parameters in an inverse manner in an easier way, the structural model should be simplified and the derived elastic dimension can be taken as the so-called comprehensive medium parameter after the characteristics of the crustal rock and many other elements are put into a comprehensive consideration. Obviously, such a parameter may deviate somewhat from the real case, yet it can ensure that the calculated result will be very close or equal to the measured one. This parameter is an important element in setting up an inverse analysis model to measure the crustal deformation and displacement in the Qinghai-Tibet Plateau. In previous models, the parameters were all appointed "empiric values", which are obviously short of theoretical proof. In the present paper, a new model is put forward to inversely analyze the physical dynamic parameters (elastic modulus and Poisson's ratio) related to various crustal medium in the plateau by means of using the displacements and boundary restraints at known node. To make the model complete, it is derived from the inversion of both the even medium and the uneven medium.

2.1 Iteration equation

The question under discussion is how to inversely obtain the material parameters included in the overall rigidity matrix when part of the restraints in the boundary area and part of displacements at the points are known. First, the error equation between the practically measured displacement and that at the finite element point is set to be

$$V = [S]\{U\} - U^0 \tag{1}$$

where V is the correction value of the measured displacement U^0, $\{U\}$ is the displacement vector at the finite point, $[S]$ is the conversion matrix, which is the sparse matrix 0,1 at the m × n step, where m is the line number of U^0 and n is the line number of $\{U\}$. The element at the point in the line vector corresponding to that in U^0 is 1 while the rest are all 0.

According to the principle of least squares method and assume that the observed displacement is equally weighted, V should meet

$$\frac{\partial(V^T V)}{\partial W} = 2V^T\left(\frac{\partial V}{\partial W}\right) = 2(SU - U^0)^T\left(S\frac{\partial U}{\partial W}\right) = 0$$

$$\text{i.e. } \left(S\frac{\partial U}{\partial W}\right)^T SU = \left(S\frac{\partial U}{\partial W}\right)^T U^0 \tag{2}$$

where w is the vector of medium parameter. Also it can be reasoned from equation (2) that the displacement at the finite element point is but a presentation of the change in the medium parameter under invariable boundary conditions.

Assume that W^k is the estimated medium parameter derived at the kth optimized iteration and that A denotes that the structural form is invariable, then the effects of different media on the displacements at the measurement points are called the sensitivity matrix at the kth iteration. Assuming that U^k is the calculated value of the systematic displacement at the kth iteration. Outspread the U^k in the neighboring W^k to a progressive form and omit the ranks above the second rank, and then

$$U^k = U^{k-1} + \frac{\partial U}{\partial W}(W^k - W^{k-1}) = U^{k-1} + A(W^k - W^{k-1}) \tag{3}$$

where $A = \frac{\partial U}{\partial W}$ is the sensitivity matrix, U^{k-1} is the calculated systematic displacement at the (k–1)th iteration and W^{k-1} is the estimated medium parameter at the (k–1)th optimized iteration.

From equations (2) and (3), we can get

$$W^k = W^{k-1} + \left[(SA)^T(SA)\right]^{-1} \cdot \left[(SA)^T U^0 - (SA)^T SU^{k-1}\right] \tag{4}$$

2.2 Inverse analysis of even medium parameters

During the inverse analysis of an even medium parameter, the key point is to get the sensitivity matrix A. For the inverse analysis in an individual region, A can be obtained by deriving the deviation coefficient of W through the principal equation $[K]\{U\}=\{P\}$ of displacement and loading, i.e.

$$A = \frac{\partial U}{\partial W} = K^{-1}\left[\frac{\partial P}{\partial W} - \frac{\partial K}{\partial W}U^{k-1}\right] \tag{5}$$

Now a few words on how to derive the deviation coefficient of a medium parameter: Assume that the medium is elastic, and then the overall rigidity matrix in the finite element analysis may be expressed as:

$$K = \int_{\Omega} B^T D B d\Omega \tag{6}$$

where B is the geometric matrix between point displacement and unit stress, D is the elastic matrix between the stress and the strain and the medium parameter vector W will include Young's modulus E and Poisson's ratio μ. Then, the derivation of W from K can be expressed as:

$$\frac{\partial K}{\partial W} = \int_{\Omega} B^T \frac{\partial D}{\partial W} B d\Omega = \int_{\Omega} B^T \begin{bmatrix} \frac{\partial D}{\partial E} \\ \frac{\partial D}{\partial v} \end{bmatrix} B d\Omega \tag{7}$$

where

$$\frac{\partial D}{\partial E} = \frac{1}{(1+\mu)(1-2\mu)} \begin{bmatrix} 1-\mu & \mu & 0 \\ \mu & 1-\mu & 0 \\ 0 & 0 & \frac{1-2\mu}{2} \end{bmatrix}$$

$$\frac{\partial D}{\partial \mu} = \frac{E}{(1+\mu^2)(1-2\mu)^2} \begin{bmatrix} 2\mu(2-\mu) & 1+2\mu^2 & 0 \\ 1+2\mu^2 & 2\mu(2-\mu) & 0 \\ 0 & 0 & -\frac{1-2\mu}{2} \end{bmatrix} \tag{8}$$

And then we can put the calculated value of sensitivity matrix A into equation (3) to get the parameter vector W of the medium.

2.3 Inverse analysis of the uneven medium parameters

First, divide the area to be calculated into several sub-areas, the division of which depends on the property and requirement of the calculation. Make the shape as regular as possible. An area of different media can be divided into several sub-areas.

For convenience without losing generality, only two non-overlapping structures are considered here, i.e.

$$\begin{cases} \Omega = \Omega_1 \cup \Omega_2 \\ \Omega_1 \cap \Omega_2 = \Gamma \end{cases} \tag{9}$$

where Γ is the bordering line (face) between regions Ω_1 and Ω_2.

After an area is finitely divided, the systematic equation can be expressed as:

$$[K]\{U\} = \{P\} \tag{10}$$

The above equation can be resolved according to the different medium parameters in different areas. The revolved systematic equation can be expressed as:

$$\begin{bmatrix} k_{11} & 0 & k_{13} \\ 0 & k_{22} & k_{23} \\ k_{13}^T & k_{23}^T & k_{33} \end{bmatrix} \begin{Bmatrix} U_1 \\ U_2 \\ U_3 \end{Bmatrix} = \begin{Bmatrix} p_1 \\ p_2 \\ p_3 \end{Bmatrix} \tag{11}$$

where U_1, U_2 and U_3 correspond to the point displacements in areas Ω_1 and Ω_2 and on bordering line (face) Γ while p_1, p_2 and p_3 correspond to the point loads in areas Ω_1 and Ω_2 and on bordering line (face) Γ, respectively.

From equation (11), it can be derived:

$$(k_{33} - k_{13}^T k_{11}^{-1} k_{13} - k_{23}^T k_{22}^{-1} k_{23}) U_3 = p_3 - k_{13}^T k_{11}^{-1} p_1 - k_{23}^T k_{22}^{-1} p_2$$

let $S_h = k_{33} - k_{13}^T k_{11}^{-1} k_{13} - k_{23}^T k_{22}^{-1} k_{23}$;

$$\bar{p}_3 = p_3 - k_{13}^T k_{11}^{-1} p_1 - k_{23}^T k_{22}^{-1} p_2$$

then we have $S_h U_3 = \bar{p}_3$ (12)

Now, the systematic equation for the finite element area can be expressed as:

$$\begin{cases} k_{11} U_1 + k_{13} U_3 = p_1 \\ k_{22} U_2 + k_{23} U_3 = p_2 \\ S_h U_3 = \bar{p}_3 \end{cases} \tag{13}$$

In area Ω_1, the following sensitivity matrix can be obtained from equation (13)

$$A = \frac{\partial U_1}{\partial W} = -k_{11}^{-1} \left[\frac{\partial k_{11}}{\partial W} U_1 + \frac{\partial k_{13}}{\partial W} U_3 + k_{13} \frac{\partial U_3}{\partial W} \right] \tag{14}$$

where the calculations of terms $\frac{\partial k_{11}}{\partial W}$, $\frac{\partial k_{13}}{\partial W}$ etc., can be carried out by referring to those in the inverse analysis on the even medium parameters. The change in parameter vector W will obviously influence the value of U_3 to be adopted. Now the key problem is the calculation of $\frac{\partial U_3}{\partial W}$.

From the third equation of equation (13), the deviation derivation of W results in:

$$\frac{\partial U_3}{\partial W} = S_h^{-1} \left(\frac{\partial \bar{p}_3}{\partial W} - \frac{\partial S_h}{\partial W} U_3 \right) \tag{15}$$

Since in area Ω_1, there are $\frac{\partial (k_{23}^T k_{22}^{-1} k_{23})}{\partial W} = 0$, $\frac{\partial (k_{23}^T k_{22}^{-1} p_2)}{\partial W} = 0$ and $\frac{\partial p_3}{\partial W} = 0$, and referring to equation (12), equation (15) can be simplified to be

$$\frac{\partial U_3}{\partial W} = S_h^{-1} \left[\left(\frac{\partial k_{13}^T}{\partial W} k_{11}^{-1} + k_{13}^T \frac{\partial k_{11}^{-1}}{\partial W} \right)(k_{13} U_3 - p_1) + \left(k_{13}^T k_{11}^{-1} \frac{\partial k_{13}}{\partial W} - \frac{\partial k_{33}}{\partial W} \right) U_3 \right] \tag{16}$$

where numerical solution may be adopted for $\frac{\partial k_{11}^{-1}}{\partial W}$, using the difference calculation to approximately replace the differential derivation, i.e.

$$\frac{\partial k_{11}^{-1}}{\partial W} = \frac{\Delta k_{11}^{-1}(\Delta W)}{\Delta W} \tag{17}$$

where ΔW denotes a minimum variable of unknown quantity W and Δk_{11}^{-1} (ΔW) the numerically calculated variable of k_{11}^{-1} corresponding to ΔW, i.e.:

$$\Delta k_{11}^{-1}(\Delta W) = k_{11}^{-1}(W + \Delta W) - k_{11}^{-1}(W) \tag{18}$$

After the value of $\frac{\partial k_{11}^{-1}}{\partial W}$ is obtained, sensitivity matrix A will be obtained, and then W^k, the new medium parameter vector can be calculated. In the same manner, the calculating equation of area Ω_2 can be derived.

To sum up, the calculating steps of the inverse analysis on uneven medium parameters can be shown in Fig. 1.

3 Inverse Analysis of the Comprehensive Medium parameters of the Plateau Crust on the Basis of GPS Velocity Field

The inverse analysis on the comprehensive medium parameter is actually that on an even medium parameter, the particular steps of which are as follows:

(1) Make out the rational value range of the comprehensive medium parameter vector W. The crustal medium parameter is normally deduced with both geological and geophysical data. According to the parameters provided by Xu Caijun, Zhang Dongning, Xu Zhonghuai (Xu, 1994; Zhang and Xu, 1994), the elastic modulus range may be assumed to be $E\in[7.5\times10^8\text{Pa}, 5.4\times10^9\text{Pa}]$ and the Poisson's ratio range be $\mu\in[0.25, 0.3]$.

(2) Divide the finite element grid.

(3) Simulate the relative kinetic velocity at the GPS points in the Qinghai-Tibet Plateau under the reference frame of Europe (Table 1), calculate the velocity at each point on the plateau boundary and take the velocity vectors of those points as loading conditions to load.

(4) Take the lower limit between the elastic modulus and Poisson's ratio as the initial value, i.e. $W_0=[7.5\times10^8, 0.25]^T$ and form up conversion matrix $[S]$ according to the requirement of equation (1).

(5) Calculate the point displacement with ANSYS5.7, and output the result.

(6) Calculate sensitivity matrix A according to equations (5)–(8).

(7) Insert sensitivity matrix A into equation (4) to get the medium parameter vector W^k after k times of iteration and calculate $\Delta W = W^k\text{-}W^{k-1}$.

(8) Theoretically, $\lim_{k\to\infty}\Delta w = 0$, but in practice, an error limit may be set for ΔW according to the precision requirement. The limit in this paper is $\Delta w\leqslant[2\%, 1\%]$. If Δw meets the above requirements, exit from the circulation, put out the result or take the result of the kth iteration as the initial value of the medium parameter vector for the next circulation and return to step 5. In this paper, the error requirement is satisfied after 6 times of iteration and the results are shown in Table 2.

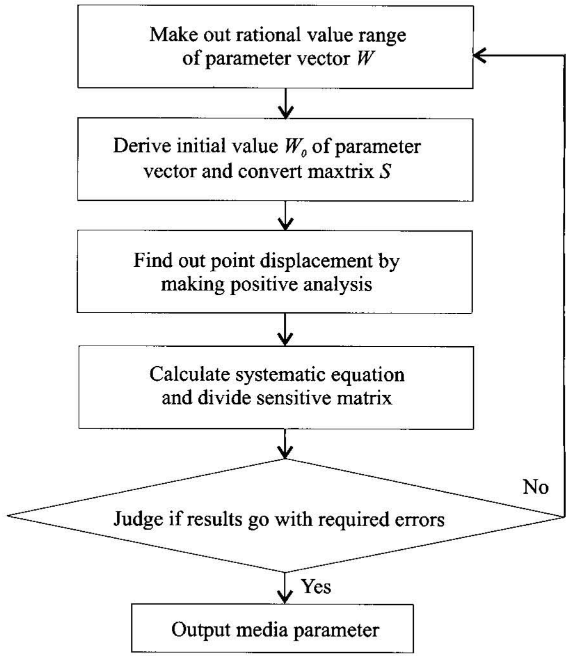

Fig. 1. Flow chart of inverse analysis on uneven medium parameters.

Table 1 Some of the GPS measured data in the Qinghai-Tibet Plateau under the reference frame of Europe

Point	Latitude (B)	Longitude (L)	Velocity in the X aspect	Velocity in the Y aspect
AYIU	39.21	101.65	−11.918	31.198
BALA	29.74	90.80	9.825	52.082
BIRA	26.48	87.26	29.186	46.051
DELI	37.38	97.73	−6.743	38.847
DUNH	40.16	94.76	−5.389	33.093
ERYU	26.12	99.99	−27.228	28.711
GOLM	36.43	94.87	−3.710	39.174
HOTA	37.12	79.93	10.538	28.067
JIRI	27.64	86.23	22.446	40.339
JIUQ	39.76	98.50	−11.980	32.495
LOBU	39.45	88.27	−2.304	29.327
MANG	37.89	91.82	−1.872	35.770
MEIG	28.33	103.14	−21.949	28.087
NEPA	28.13	81.57	29.400	42.567
POKH	28.20	83.98	25.853	41.292
SANC	39.95	78.44	9.388	31.088
SHIQ	32.51	80.10	6.250	37.811
SIMI	29.97	81.83	16.058	39.006
SOXI	31.89	93.78	−3.028	55.418
TUOT	34.21	92.45	−5.896	54.680
WUQO	39.70	75.12	7.298	28.313
XIAL	31.30	100.75	−19.196	43.922
XIGA	29.25	88.86	13.956	48.630
XINI	36.66	101.65	−8.565	38.879

Table 2 Iterative results of the integrated medium parameters

Iterative time	Elastic module E (GPa)	Poisson's ratio μ	Error of E ($\Delta E/E$)	Error of μ ($\Delta\mu/\mu$)
1	0.75	0.25		
2	1.61545	0.26124	53.6%	4.3%
3	2.78924	0.26597	42.1%	1.78%
4	3.68547	0.26978	24.3%	1.41%
5	4.16529	0.26991	11.5%	0.48%
6	4.20246	0.26991	0.88%	0.00%

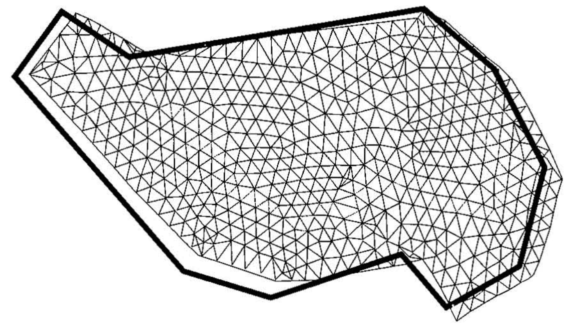

Fig. 2. The integral stractural deformation of the plateau.

4 Simulation on the Crustal Deformation of the Qinghai-Tibet Plateau

To make out the general kinetic trend and the distribution of structural stress field in the Qinghai-Tibet Plateau, it is necessary to take the whole plateau as one body to simulate. From the GPS surveyed data, those who are fairly even and able to reflect the kinetic characteristics of the plateau (see Table 1) are selected to be the deformation data to be loaded and the results of the 6th iteration in Table 2 are chosen to be the comprehensive medium parameter of the plateau crust. The model cell adopts the triangular cell in the shell of three points and the thickness of the shell is selected at 35 km.

Based on the above, the overall kinetics of the Qinghai-Tibet Plateau is simulated. The result shows that the overall crust of the plateau shows a trend of north-south compression and east-west sliding. In Fig. 2, the bold line reflects the state before the deformation. Fig. 3 shows the integral structural deformation vector of the plateau. Since the Indian plate has been subducted from

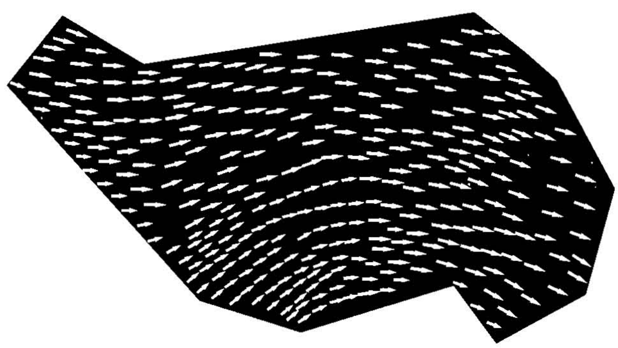

Fig. 3. The integral structural deformation vector of the plateau.

Table 3 List of the strain components and strain characteristic parameters of the plateau

Point No.	Longitude L	Latitude B	EPTOX	EPTOY	EPTOXY	EPTOINT	EPTOEQV
2	73.694	39.810	0.40631	−0.49325	−0.50398	1.03110	0.89617
9	77.491	39.922	0.61969	−0.13770	0.209610	0.81219	0.79935
19	81.830	29.970	0.246340	−1.57970	0.829590	2.16270	2.08860
27	79.558	30.164	0.095926	−0.60198	0.872960	1.11760	1.06330
65	78.470	32.498	0.294720	−0.04080	−0.38695	0.51216	0.49550
78	77.428	34.812	0.08892	0.194890	−0.73356	0.74118	0.68772
96	89.158	39.060	1.38850	−0.85515	−2.16560	3.11830	2.74010
138	84.786	38.778	0.19115	−0.35313	−1.64310	1.73090	1.50560
168	86.280	37.873	0.35960	−0.75620	−3.34190	3.52320	3.07060
194	84.112	31.398	1.14550	−2.19930	−0.48392	3.37970	3.06710
216	85.158	36.295	1.11310	−1.27190	−2.68240	3.58930	3.11150
253	101.02	37.280	0.097629	−0.21372	−1.71510	1.74310	1.51300
305	92.760	37.240	0.161710	−0.36530	−3.36740	3.40840	2.95710
344	73.941	42.516	0.632520	−3.32320	0.002941	4.31840	4.14890
380	91.702	38.875	0.256320	−0.82449	−1.98270	2.25810	2.01710
400	87.113	27.142	1.88680	−4.57990	−1.58760	6.65870	6.22420
434	90.632	33.191	2.801700	−4.60620	−1.00270	7.47550	6.66150
487	100.82	29.966	-0.37218	0.247090	2.351500	2.43170	2.10870
510	97.799	42.113	2.70810	4.010300	−13.9050	13.96600	13.43300
530	104.23	34.324	-0.05560	0.623160	−0.67399	0.97198	0.96435

the south, it results in the violent structural compressive deformation and inland subduction in the southern part of the plateau. The compressive stress gradually decreases towards the northern part of the plateau, and it is resisted by the Tarim lithospheric root, making the deformation characteristics change from the inland subduction to the shortening and vertical thickening of the crust, so that the displacement shows a trend of deducing from south to north. It can also be seen from Figs. 4 and 5 that the east-west differential movement within the plateau is uneven and the stretch vector is much larger towards the east than the west. Figures 4 and 5 show that the plateau is dominated by moving towards the east. It should be noted that, starting from the main collision belt along the Himalayas, the stretch vector of the plateau trends to decrease gradually towards the east, indicating that the eastward movement of the crust-mantle materials of the plateau weakens gradually. This might have resulted from the growth of the east-west sliding faults within the plateau, which have gradually absorbed the above movement vector and turned it into sliding deformation.

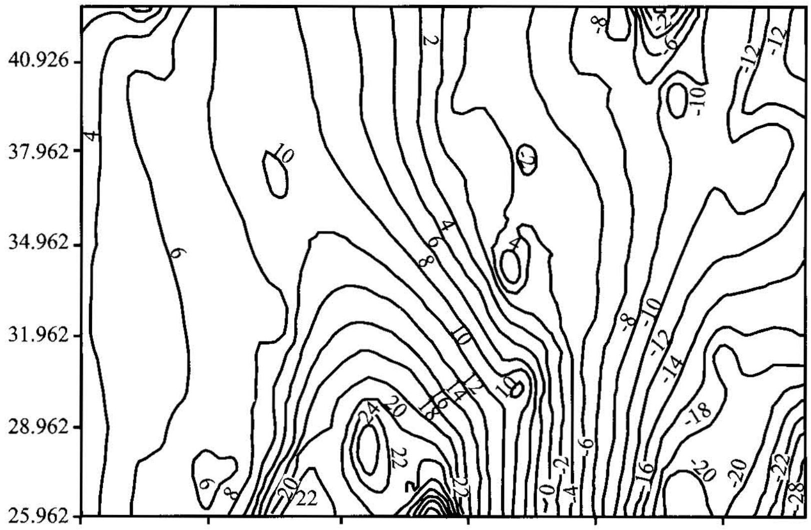

Fig. 4. Isoline diagram of the velocity field in the X aspect.

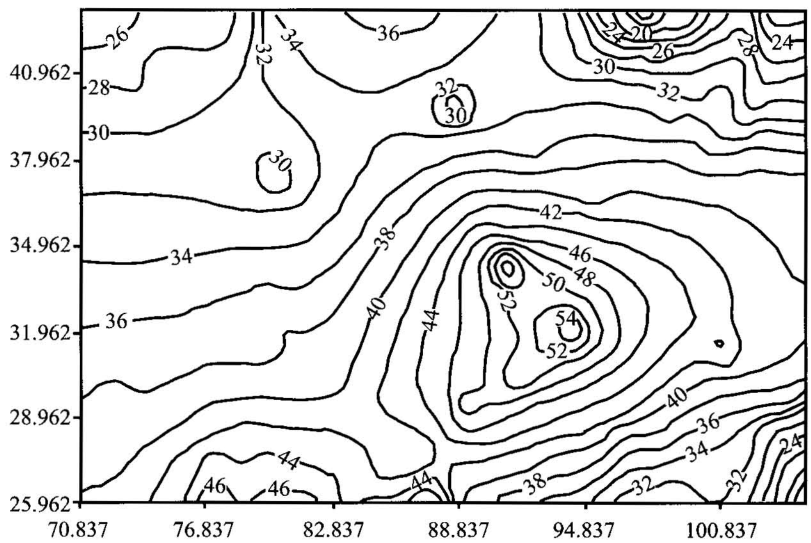

Fig. 5. Isoline diagram of the velocity field in the Y aspect.

The structural deformation of the plateau is dominated by the north-south compressive stress, accompanied with the east-west extensional strain, as is fully reflected by the data in Table 3. Table 3 lists the strain components and equivalent strain values of the plateau, where EPTOX and EPTOY represent the strain components of the X aspect (east to west) and the Y aspect (north to south), respectively, while EPTOINT and EPTEQV represent the strain intensity and the equivalent strain, respectively. Apparently, there are more positive EPTOX values, indicating that extension dominates in the east to west aspect, while the EPTOY values are basically negative, indicating that compression prevails in the north to south aspect. This goes well with the present explanation about the tectonic movement of the plateau.

Corresponding to the strain field is the distribution of principal stresses on the earth surface of the area under study. Figure 6 shows the equivalent principal stress contour lines, giving a clearer picture of the structural stress field in the whole area of the plateau.

To show the structural deformation in the plateau more directly, the simulated result of the overall movement in the plateau has been turned into an animated cartoon file, making the structural deformation more vivid.

5 Conclusions

At present, in the explanation on the geodynamics or physics of the Qinghai-Tibet Plateau, the geodetic surveyed materials obtained at a proper density in a fairly large scope are based on spatially observed materials with the help of GPS, i.e. the displacement materials. Thus, different from the geophysical inverse simulation, it is unnecessary to set up various basic equations and their solution conditions. Apparently, the explanation on the

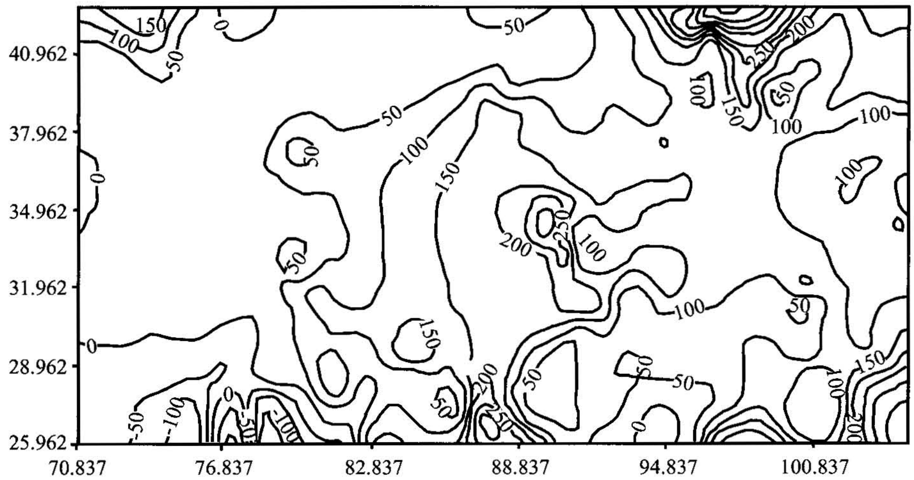

Fig. 6. Distribution of the principal stress contours.

geodetic surveyed deformation mainly aims at some physico-dynamic parameters, structural stress fields and boundary forces in the earth or on its surface to create an organic relationship between the displacement data and the crustal physico-dynamic parameter or the force leading to the deformation.

Focusing on the measurement of the crustal deformation in the Qinghai-Tibet Plateau and the related explanation, the research of this paper can be concluded as:

(1) A displacement inverse analysis for the material parameter is put forward and inversely analyzed. The resulted elastic modulus goes well with the deduction from the present geological and geophysical data with a nearly equal Poisson's ratio. This further supports the rationality of the model.

(2) The overall structural deformation of the Qinghai-Tibet Plateau is simulated and the resulted values are animatedly cartooned. The results go well with the explanation on the present tectonic movement of the plateau. The present tectono-dynamic characteristics of the plateau are the result of combined actions of the neighboring rigid platforms, i.e. the Indian, Tarim, North China and Yangtze platforms, with the help of relative sliding between the different plates within the plateau. The major force comes from the south, i.e. the northward subduction of the Indian plate is active while that of Tarim, North China and Yangtze is passive.

(3) The present structural stress field is dominated by north-south compressive stress accompanied with east-west extensional stress, which is closely related to the northward compression of the Indian plate and the southward advance of the Eurasian plate. Therefore, we can say that the present structural stress field of the plateau is under the control of the mutual collision between the Eurasian plate and Indian plate.

The research of the paper indicates as there lack sufficient observation data, the explanation on the structural deformation of the Qinghai-Tibet Plateau is obviously limited. Therefore, it will be of great significance for further exploration into the mechanism of the structural deformation of the plateau if we further improve the geodetic measurement system of the plateau so as to monitor in real-time the dynamic deformation of the plateau, especially near the explored fault zones, and prefect the 3-D or even 4-D dynamic model of the plateau.

Acknowledgements

The research results are part of a project carried out in 1999–2002 and financially supported by the US National Foundation (No. ASF EARO125968), in 2001–2003 and financially supported by the National Natural Science Foundation of China (Nos. 40271089) and the Major Sci-Tech Research Project of the Ministry of Education.

Manuscript received Jan. 18, 2004
accepted June 21, 2004
edited by Zhu Xiling

References

Armijo, R., Tapponnier, P., Mercier, J.L., and Han, T.L., 1986. Quaternary extension in Southern Tibet: Field observations and tectonic implication. *J. Geophys. Res.*, 91: 803–872.

Bilham, R., Larson, K., Freymueller, J., and Project Idylhim Members, 1997. GPS measurements of present day convergence rates across the Nepal Himalaya. *Nature* 386: 61–64.

Blisniuk, P.M., Siwen, S., Kuchel, O., and Ratschbacher, L., 1998. Late Neogene extension in the Shuang Hu graben, central Tibet. *Eos Trans. AGU*, 74–79.

Gao Yongfeng, Hou Zengqian, Wei Ruihua and Zhao Rongsheng, 2003. Post-collisional adskitic porphyries in Tibet geochemical and Sr-Nd-Pb isotopic constraints on partial melting of oceanic lithosphere and crust-mantle interaction. *Acta Geologica Sinica* (English edition), 77(2): 194–203.

Hou Zengqian, Chen Wen and Lu Jian, 2002. Collision event during 177–135 Ma on the eastern margin of the Qinghai-Tibet Plateau: Evidence from $^{40}Ar/^{39}Ar$ dating for basalts on the western margin of the Yangtze platform. *Acta Geologica Sinica* (English edition), 76(2): 194–204.

Jin Shuanggen and Zhu Wenyao, 2003. Active motion of tectonic blocks in East Asia: Evidence from GPS measurement. *Acta Geologica Sinica* (English edition), 77(1): 59–63.

Sino-British Comprehensive Geological Investigation Team of the Qinghai-Tibet Plateau, 1990. *Geological Evolution of the Qinghai-Tibet Plateau.* Beijing: Science Press, 30–40.

Wu Zhenhan, Hu Daogong, Ye Peisheng, Zhao Xun and Liu Qisheng, 2004. Thrusting of the north Lhasa block in the Tibetan Plateau. *Acta Geologica Sinica* (English edition), 78(1): 246–259.

Yang Xiaosong, Ma Jin, Jin Zhenmin, Gao Shan and Ma Shengli, 2003. Partial melting and its implications for understanding the seismic velocity structure within the southern Tibetan crust. *Acta Geologica Sinica* (English edition), 77(1): 64–71.

Yang Yuanxi, 1991. Analysis model of diastrophism. *Journal of Institute of Surveying and Mapping*, 17(2): 98–102.

Yang Zhiqiang and Ju Tianyi, 1999. Collocation and field work plan about the crustal GPS monitoring system of local areas of the Himalayas. *J. Northwest Univ.*, (6): 83–86.

Wang Ren, 1989. Some dynamic questions in geotectonic analysis. *Advances in Mechanics*, 19(2): 128–130.

Wang Suyun, Xu Zhonghuai, Yu Yanxiang and Zhang Lin, 1996. Inversion for the plate driving forces acting at the boundaries of China and its surroundings. *Acta Geophysica Sinica*, 39(6): 764–771.

Xun Caijun, 1994. The Kinematic Models of Crustal Movement and Tectonic Stress Field in the Tibetan Plateau. Ph.D. Dissertation of Wuhan University.

Yan Renjun, Gongpu and HuangYuying, 1998. Back analysis calculation of inhomogeneous material based on domain decomposition method. *Journal of Wuhan Transportation University*, 22(3): 277–279.

Zhang Dongning and Xu Zhonghuai, 1994. Status of modern tectonic stress field in the Tibetan Plateau and numerical simulation of tectonic movement. *Earthquake Research in China*, 10(2): 58–62.